



**HAL**  
open science

# Phototransformation of Three Psychoactive Drugs in Presence of Sedimental Water Extractable Organic Matter

Cristina Jiménez-Holgado, Vasilios Sakkas, Claire Richard

► **To cite this version:**

Cristina Jiménez-Holgado, Vasilios Sakkas, Claire Richard. Phototransformation of Three Psychoactive Drugs in Presence of Sedimental Water Extractable Organic Matter. *Molecules*, 2021, 26 (9), pp.2466. 10.3390/molecules26092466 . hal-03265713

**HAL Id: hal-03265713**

**<https://hal.science/hal-03265713>**


Submitted on 21 Jun 2021

**HAL** is a multi-disciplinary open access archive for the deposit and dissemination of scientific research documents, whether they are published or not. The documents may come from teaching and research institutions in France or abroad, or from public or private research centers.

L'archive ouverte pluridisciplinaire **HAL**, est destinée au dépôt et à la diffusion de documents scientifiques de niveau recherche, publiés ou non, émanant des établissements d'enseignement et de recherche français ou étrangers, des laboratoires publics ou privés.

## Article

# Phototransformation of Three Psychoactive Drugs in Presence of Sedimental Water Extractable Organic Matter

Cristina Jiménez-Holgado <sup>1,2</sup>, Vasilios Sakkas <sup>1</sup> and Claire Richard <sup>2,\*</sup> 

<sup>1</sup> Laboratory of Analytical Chemistry, Department of Chemistry, School of Sciences, University of Ioannina, 45110 Ioannina, Greece; crijimhol@gmail.com (C.J.-H.); vsakkas@uoi.gr (V.S.)

<sup>2</sup> Institute of Chemistry of Clermont-Ferrand, Université Clermont Auvergne, CNRS, SIGMA-Clermont, ICCF, F-63000 Clermont-Ferrand, France

\* Correspondence: claire.richard@uca.fr

**Abstract:** Psychoactive drugs are classified as contaminants of emerging concern but there is limited information on their fate in surface waters. Here, we studied the photodegradation of three psychoactive drugs (sertraline, clozapine, and citalopram) in the presence of organic matter (WEOM) extracted under mild conditions from sediment of Lake Pamvotis, Greece. Spectral characterization of WEOM confirmed its humic-like nature. Preliminary experiments using chemical probes showed that WEOM was able to produce oxidant triplet excited state (<sup>3</sup>WEOM\*), singlet oxygen (<sup>1</sup>O<sub>2</sub>), and hydroxyl radicals under irradiation with simulated solar light. Then, WEOM at 5 mgC L<sup>-1</sup> was irradiated in the presence of the three drugs. It enhanced their phototransformation by a factor of 2, 4.2, and 16 for sertraline, clozapine, and citalopram, respectively. The drastic inhibiting effect of 2-propanol (5 × 10<sup>-3</sup> M) on the reactions demonstrated that hydroxyl radical was the key intermediate responsible for drugs photodegradation. A series of photoproducts were identified by ultra-high performance liquid chromatography (UHPLC) coupled to high resolution mass spectrometry (HR-MS). The photodegradation of the three drugs proceeded through several pathways, in particular oxidations of the rings with or without O atom inclusion, N elimination, and substitution of the halogen by OH. The formation of halogenated aromatics was observed for sertraline. To conclude, sedimental natural organic matter can significantly phototransform the studied antidepressant drugs and these reactions need to be more investigated. Finally, ecotoxicity was estimated for the three target analytes and their photoproducts, using the Ecological Structure Activity Relationships (ECOSAR) computer program.

**Keywords:** antidepressants; sediment; photodegradation; water extractable organic matter; photoproducts



**Citation:** Jiménez-Holgado, C.; Sakkas, V.; Richard, C.

Phototransformation of Three Psychoactive Drugs in Presence of Sedimental Water Extractable Organic Matter. *Molecules* **2021**, *26*, 2466.

<https://doi.org/10.3390/molecules26092466>

Academic Editor: Wanhong Ma

Received: 25 March 2021

Accepted: 16 April 2021

Published: 23 April 2021

**Publisher's Note:** MDPI stays neutral with regard to jurisdictional claims in published maps and institutional affiliations.



**Copyright:** © 2021 by the authors. Licensee MDPI, Basel, Switzerland. This article is an open access article distributed under the terms and conditions of the Creative Commons Attribution (CC BY) license (<https://creativecommons.org/licenses/by/4.0/>).

## 1. Introduction

Psychoactive drugs are widely used to treat diseases such as depressive symptoms and social anxiety disorder. This is due to the lack of regulation, together with the ignorance of their fate and the absence of effective methods of elimination, these drugs have been classified as contaminants of emerging concern (CECs). The increasing consumption of these compounds in developed countries enhances in fact the risk of environmental contamination and adverse effects on human health and habitats [1]. They enter the aquatic environment mainly through hospital effluents and wastewater treatment plants and, being poorly degradable by traditional biological processes, they are present in relative high amounts in water bodies and sediments. The psychoactive drugs sertraline (SER), citalopram (CIT), and clozapine (CLO) were detected between 13.2 ng L<sup>-1</sup> to 15.0 µg L<sup>-1</sup> in wastewater treatment plants effluents, 8.9 ng L<sup>-1</sup> to 30.0 µg L<sup>-1</sup> in fresh waters, and 14.4 to 71.9 ng.g<sup>-1</sup> in river sediments [2–4]. Once released in the aquatic environment, these compounds can undergo chemical reactions and generate new chemicals, that might also be harmful and therefore need to be identified. Although there is no consistent literature data on the ecotoxicity of these compounds, it has been found that acute and chronic exposure

of SER and CIT show effects on algae [5], crustaceans [6–8], bivalves [9,10] and fish [11]. As well, Villain et al. classified these 3 drugs as class 1 toxicity, where metabolites should be analyzed in priority and the ecotoxicity can be estimated with QSAR models [12]. Calza et al. has found that after 20 min of solar light irradiation, SER and its photoproducts, in the presence of TiO<sub>2</sub> display higher acute toxicity potential (based on ECOSAR software) [13].

The degradation of these psychoactive drugs can be induced by solar light because they absorb solar radiations between 295 and 450 nm (Figure 1A). According to the literature data, irradiation with simulated solar light in pure water yielded a half-life of 65 d for CIT [14], 8 h for CLO [4] and between 6 min at pH 12 and > 1 h at pH 5 for SER [15]. The phototransformation of SER and CIT were also reported to be sensitized by the natural organic matter, NOM, present in surface water [13–16]. Indeed, NOM that contains humified light-absorbing compounds can photoinduce the degradation of chemicals through the generation of reactive species such as hydrogen peroxide (H<sub>2</sub>O<sub>2</sub>) and superoxide radical anion (O<sub>2</sub><sup>-</sup>) [17], <sup>1</sup>O<sub>2</sub> [18,19], oxidant triplet excited state (<sup>3</sup>NOM\*) [20], and hydroxyl radical (HO·) [21–23].

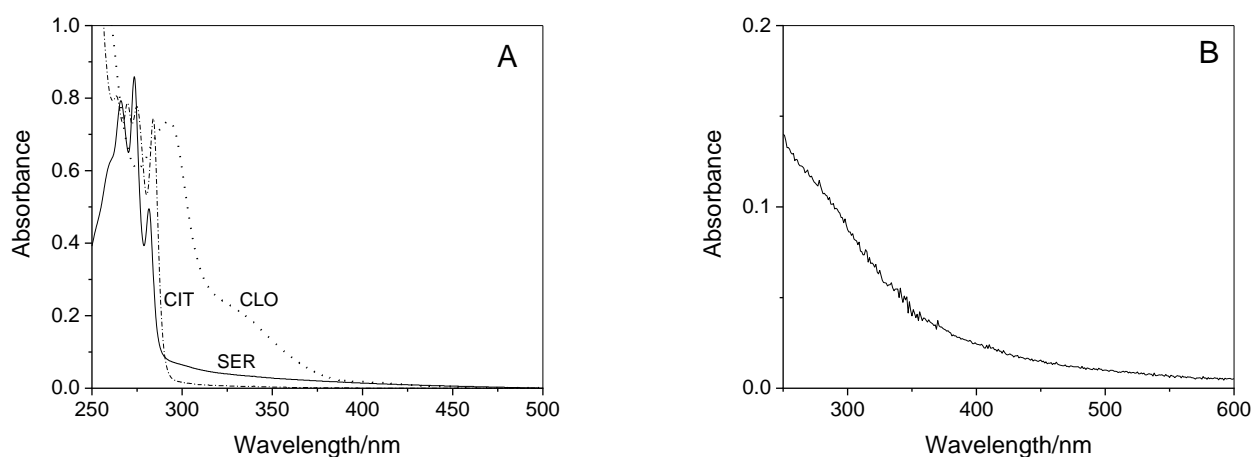


**Figure 1.** UV-vis absorption of sertraline (SER), clozapine (CLO) and citalopram (CIT) at 5 ppm in water at pH 7 (A) and WEOM (18 mgC L<sup>-1</sup>) at pH 9.2 (B).

Part of NOM present in the water column of lakes and rivers comes from sediments resolubilization. Sediments are formed by accumulation of deposited particulate organic matter, that undergoes biochemical transformations [24]. Sediment organic matter generally contains a high proportion of humified compounds and can potentially sensitize the photodegradation of aquatic contaminants. The water-soluble sediment organic matter can be recovered by sampling the sedimental pore water [25], or by extraction from sediment using neutral or slightly alkaline water as described for soils [26].

In this work, we aimed to better understand the fate of SER, CLO and CIT psychoactive drugs when irradiated in the presence of natural organic matter extracted from the Lake Pamvotis (Ioannina, NW Greece) sediment. The water soluble sedimental organic matter (WEOM), beforehand extracted with water under mild conditions, was first characterized by spectral techniques to confirm its humic-like nature. Then, using the scavenging technique, we investigated its capacity to generate reactive species (<sup>3</sup>WEOM\*, <sup>1</sup>O<sub>2</sub> and HO·) to finally demonstrate the important role of HO· in the photodegradation of the three drugs. The drugs photoproducts were identified by means of UHPLC-HR-MS and photodegradation pathways were proposed. A toxicity assessment was followed based on the ECOSAR computer model for the parent molecules and their by-products.

## 2. Results and Discussion

### 2.1. Main Characteristics of the Sediments

Sediment was analyzed prior to drugs adsorption measurements. The sediment particle size was found to be equal to 100 ± 10 µm and the percentage of organic matter to

$1.91 \pm 0.02\%$  of the dry matter. In the literature, the averaged grain size and organic matter content in lake, river and sea sediments vary between silt (2–500  $\mu\text{m}$ ) and clay (<2  $\mu\text{m}$ ) composition, and contain between 0.37–8.0% of organic matter [27]. Lake Pamvotis is a shallow, closed and eutrophic Mediterranean Lake with ecological significance [28,29]. This lake has been shown to exist since the Pleistocene period [30]. In a previous work, the organic matter content in Lake Pamvotis sediments was found to vary between 4.8% and 15.3%, where the lowest content was found in the coarser sandy sediments and the highest in the silt-clay portion [31]. Our sediments showed a grain size larger than that of previous studies, and the organic matter content obtained was therefore lower, in agreement with previous publications [32,33].

## 2.2. Extraction and Characterization of WEOM from Sediments

By stirring sediment (120 g  $\text{L}^{-1}$ ) in pH 9.2 water during 5 d, we could recover WEOM. The DOC content of the WEOM solution was of 18  $\text{mgC L}^{-1}$ . WEOM showed the typical UV-visible absorption spectrum of humic-like substances with an exponentially decreasing absorption extending up to 600 nm with a shoulder around 280 nm (Figure 1B).  $\text{SUVA}_{254}$  was equal to 0.44  $\text{L}\cdot\text{mg}^{-1}\cdot\text{m}^{-1}$ ,  $S_{275-295}$  to 0.0105  $\text{nm}^{-1}$  and  $E_2/E_3$  to 3.41. From the  $\text{SUVA}_{254}$  and  $E_2/E_3$  values, we could estimate that the percentage of aromaticity was equal to 6.5% and the average Mw to 1.7 kDa. These data that characterize an organic matter moderately aromatic with an overall small molecular weight are in line with those of other sediment organic matters [25,34]. Among main ions detected in Lake Pamvotis, nitrate was the highest concentrated. UHPLC-MS analysis revealed that nitrate ( $m/z = 61.9873$  at  $\pm 5$  ppm) was present in WEOM at a concentration  $< 5 \times 10^{-5}$  M, therefore too low for a significant photochemical effect.

The three-dimensional fluorescence spectrum of WEOM contained peaks A and C, assigned as UVC and UVA humic-like fluorophores, respectively, and peaks T assigned as protein tryptophan-like fluorophores (Figure 2) [35]. All these spectral characteristics confirmed the humic-like nature of WEOM. The values of fluorescence indices FI (1.47) and BIX (0.79) that represent the relative contribution of terrestrial and microbial DOM sources and the relative contribution of autochthonous natural organic matter, respectively, indicated that sediments from Lake Pamvotis had a terrestrial contribution, as supported by previous publications [36].

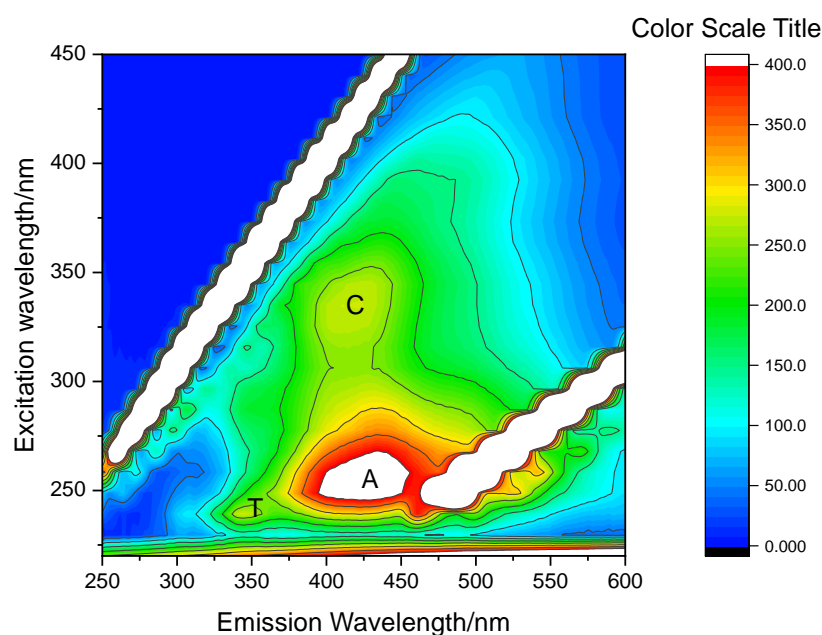


**Figure 2.** Three dimensional fluorescence spectrum of WEOM ( $18 \text{ mgC L}^{-1}$ ) at pH 9.2.

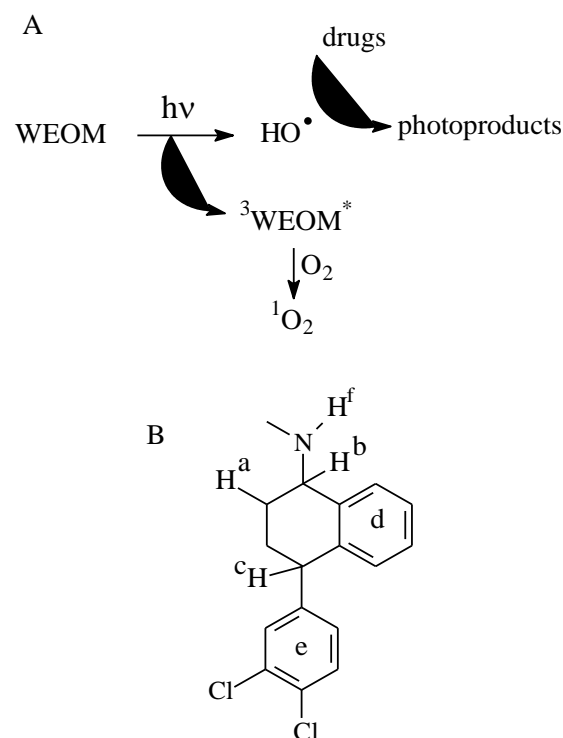
### 2.3. Photoproduction of Reactive Species upon WEOM Irradiation

Three chemical probes (2,4,6-trimethylphenol, furfuryl alcohol and terephthalic acid) were used to evidence the production of photooxidants  $^3\text{WEOM}^*$ ,  $^1\text{O}_2$  and  $\text{HO}^\bullet$ , respectively [37]. While it is photostable when irradiated alone, 2,4,6-trimethylphenol ( $5 \times 10^{-6}$  M) disappeared in the presence of WEOM ( $5 \text{ mgC L}^{-1}$ ) at circumneutral pH in accordance with the formation of  $^3\text{WEOM}^*$  (Supplementary Figure S3). The apparent first order rate constant of reaction  $k$  was equal to  $0.020 \pm 0.002 \text{ min}^{-1}$  (Supplementary Figure S1). The quantum yield coefficient of the phenol photodegradation  $f_{\text{TMP}}$  was equal to  $k/R_a^{\text{WEOM}}$ , where  $R_a^{\text{WEOM}}$  was the rate of light absorption by WEOM in the reactor. One found  $f_{\text{TMP}} = 46 \pm 5 \text{ M}^{-1}$ , a value falling in the range of those reported for other NOMs [38].

WEOM was also expected to generate  $^1\text{O}_2$  because this species is produced from the deactivation of  $^3\text{WEOM}^*$  by oxygen. The loss of furfuryl alcohol ( $5 \times 10^{-5}$  and  $10^{-4}$  M) upon irradiation in the presence of WEOM ( $5 \text{ mgC L}^{-1}$ ) confirmed this hypothesis (Supplementary Figure S2). From the  $k$  value ( $0.0011 \pm 0.0002 \text{ min}^{-1}$ ), one could estimate the quantum yield of  $^1\text{O}_2$  formation,  $\Phi_{\text{SO}}$ , using the simplified relationship:  $\Phi_{\text{SO}} = \alpha_{\text{FFA}} \times k \times (\text{Furfuryl alcohol})/R_a^{\text{WEOM}}$ , where  $\alpha_{\text{FFA}}$  is the fraction of  $^1\text{O}_2$  scavenged by furfuryl alcohol. Considering that  $^1\text{O}_2$  reacts with furfuryl alcohol with a bimolecular rate constant of  $1.2 \times 10^8 \text{ M}^{-1} \text{ s}^{-1}$  [39] and is deactivated in water with a monomolecular rate constant of  $2.5 \times 10^5 \text{ s}^{-1}$  [40], it comes that  $\alpha_{\text{FFA}}$  was equal to 2.3% and 4.6% by furfuryl alcohol at  $5 \times 10^{-5}$  and  $10^{-4}$  M, respectively. This gives  $\Phi_{\text{SO}} = 0.055 \pm 0.010$ , a value in the upper limit of those reported for aquatic NOMs [19].

We also irradiated terephthalate ( $10^{-5}$  M) in the presence of WEOM ( $5 \text{ mgC L}^{-1}$ ) at pH = 7. As expected, we observed the formation of the fluorescent hydroxylated photoproduct resulting from the reaction between terephthalic acid and  $\text{HO}^\bullet$  radicals ( $4.4 \times 10^9 \text{ M}^{-1} \text{ s}^{-1}$  [41]) (Supplementary Figure S3). Using a calibration curve (Supplementary Figure S3), one could determine that the hydroxylated photoproduct was formed at a rate of  $(5.9 \pm 0.6) \times 10^{-11} \text{ M s}^{-1}$  during the first 40 min of the reaction.

Therefore, as for other NOMs of water and soils, WEOM of Lake Pamvotis sediment was able to generate photooxidants under simulated solar light irradiation (Scheme 1A).



**Scheme 1.** Reactive species production from WEOM (A) and chemical structure of SER (B).

#### 2.4. Irradiation of Drugs in the Presence of WEOM

The drugs ( $5 \times 10^{-6}$  M) were first irradiated in pH 7 buffered purified water to measure their rate of direct photolysis. Plots of  $\ln C/C_0$  vs. irradiation time are presented in Figure 3A–C. The rate constants deduced from these linear plots ( $k_{\text{direct photolysis}}$ ) were of  $(1.6 \pm 0.2) \times 10^{-5}$ ,  $(0.60 \pm 0.03) \times 10^{-5}$  and  $(1.3 \pm 0.1) \times 10^{-6}$  s $^{-1}$  for SER, CLO and CIT, respectively (Figure 3D and Supplementary Table S1). This order of photoreactivity is consistent with the literature data, where SER was reported to be faster photolyzed than the two other drugs [4,14,15].

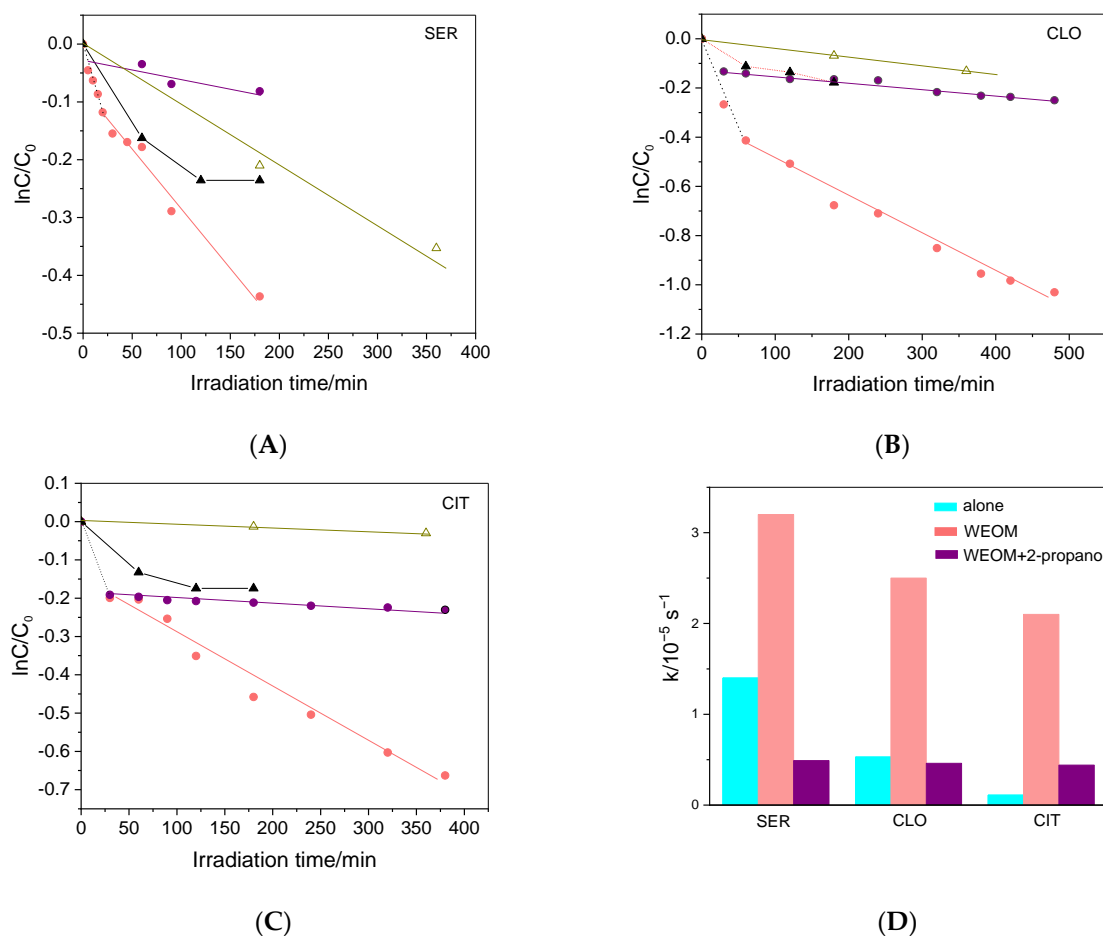


**Figure 3.** Photodegradation of SER (A), CLO (B) and CIT (C) ( $5 \times 10^{-6}$  M) in purified water buffered at pH 7 ( $\Delta$ ), in the presence of WEOM ( $5 \text{ mgC L}^{-1}$ ) ( $\bullet$ ) and in the presence of WEOM ( $5 \text{ mgC L}^{-1}$ ) and 2-propanol ( $5 \times 10^{-3}$  M) ( $\blacklozenge$ ). Dark control experiments ( $\blacktriangle$ ). Apparent first order of disappearance of drugs in different conditions (D).

Then, drugs were irradiated in the presence of WEOM ( $5 \text{ mgC L}^{-1}$ ) (Figure 3A–C). For all of them, the plot of  $\ln C/C_0$  vs. irradiation time presented two parts. The slope of the first linear part (between 0 and 20 to 50 min) was higher than that of the second linear part. Such a two-part photodegradation curve was neither observed with 2,4,6-trimethylphenol (Supplementary Figure S1) nor with furfuryl alcohol (Supplementary Figure S2). Dark control experiments revealed that drugs disappeared even in the absence of light—likely by adsorption on the small particles  $< 0.45 \mu\text{m}$  present in WEOM solutions filtrated with  $0.45 \mu\text{m}$  filters. Accordingly, the three drugs showed significant adsorption on the sediment (Supplementary Figure S4). Therefore, the first part of the plots was not taken into account for the kinetic study and the rate constants  $k$  were extracted from the second part of the plots exclusively. The  $k$  values in the presence of WEOM varied between  $2.1$  and  $3.5 \times 10^{-5} \text{ s}^{-1}$  (Figure 3D). In the presence of WEOM, drugs were supposed to



disappear by direct photolysis and by WEOM-mediated photodegradation and  $k$  was thus equal to:

$$k = k_{\text{direct photolysis}^*} + k_{\text{WEOM}}$$

where  $k_{\text{direct photolysis}^*}$  was  $k_{\text{direct photolysis}}$  after correction for the screen effect of WEOM (SI, Text 1), and  $k_{\text{WEOM}}$  is the rate constant due to the sole contribution of WEOM. Values of  $k_{\text{WEOM}}$  were obtained by subtracting  $k_{\text{direct photolysis}^*}$  from  $k$ . Values of  $k_{\text{WEOM}}$  varied within a very narrow range ( $1.8\text{--}2.0 \times 10^{-5} \text{ s}^{-1}$ ) (Supplementary Table S1) in line with an important contribution of HO· radical in the reactions because these radicals show poor specificity and were expected to oxidize the three drugs at the same rate.

To confirm the involvement of HO· radical, drugs were irradiated in the presence of WEOM ( $5 \text{ mgC L}^{-1}$ ) and 2-propanol ( $5 \times 10^{-3} \text{ M}$ ) used as an HO· radical quencher ( $k_{\text{HO}} = 1.9 \times 10^9 \text{ M}^{-1} \text{ s}^{-1}$  [42]). All the rates of disappearance were drastically reduced (Figure 3A–C) and for each drug the rate constant obtained in the presence of WEOM and 2-propanol ( $k_{2\text{-propanol}}$ ) approached  $k_{\text{direct photolysis}^*}$  indicating the very high contribution of HO· radical in the WEOM photosensitized reaction (Figure 3D, Supplementary Table S1). In the case of SER,  $k_{2\text{-propanol}}$  was even lower than  $k_{\text{direct photolysis}^*}$ .

### 2.5. Drugs Photoproducts

Photoproduct analysis was performed on neutral solutions of drugs ( $5 \times 10^{-6} \text{ M}$ ) and WEOM ( $5 \text{ mgC L}^{-1}$ ) irradiated for 8 h until drugs conversion between 33% and 69%. UHPLC-MS data are compiled in Tables 1–3 while main pathways deduced from MS data are given in Figure 4.

**Table 1.** HRMS data of the main photoproducts of SER after 8 h of irradiation in the presence of WEOM. Percentage of conversion = 69%.

Peak Code	Elemental Formula of $[M + H]^+$	$m/z$	TIC Peak Area	Chemical Modifications vs. SER
SER	$C_{17}H_{18}Cl_2N$	306.0803 308.0771 310.0734		
SER-1 Several peaks	$C_{17}H_{18}Cl_2NO$	322.0753 324.0722 326.0687	$3.2 \times 10^8$	SER + O fragment M – H <sub>2</sub> O
SER-1bis Several peaks	$C_{17}H_{18}Cl_2NO$	322.0753 324.0722 326.0687		SER + O
SER-2 Several peaks	$C_{17}H_{18}Cl_2NO_2$	338.0699 340.0670 342.0641	$1.7 \times 10^7$	SER + 2O fragment M – H <sub>2</sub> O for some of the peaks
SER-3 2 peaks	$C_{17}H_{16}Cl_2N$	304.0647 306.0615 308.0581	$4.3 \times 10^7$	SER – 2H
SER-4	$C_{16}H_{13}Cl_2O$	291.0330 293.0300 295.0266	$9.8 \times 10^7$	SER – CH <sub>3</sub> NH <sub>2</sub> + O
SER-5 2 peaks	$C_{17}H_{19}ClNO$	288.1146 290.1110	$3.7 \times 10^7$	SER – Cl + OH
SER-6	$C_{17}H_{20}NO_2$	270.1481	$1.8 \times 10^6$	SER – 2Cl + OH + OH
SER-7	$C_{16}H_{14}ClO$	257.0721 259.0690	$1.8 \times 10^7$	SER – CH <sub>3</sub> NH <sub>2</sub> + O – Cl + H
	Elemental formula of $[M-H]^+$	$m/z$	TIC peak Area	Chemical modifications vs. SER
SER-8	$C_6H_3Cl_2O$	160.9553 162.9524 164.9495	$5.7 \times 10^6$	3,4-dichlorophenol
SER-9	$C_7H_3Cl_2O_2$	188.9507 190.9275 192.9279	$2.6 \times 10^6$	3,4-dichlorobenzoic acid

**Table 2.** HR-MS data of the main photoproducts of CLO after 8 h of irradiation in the presence of WEOM. Percentage of conversion = 44%.

Peak Code	Elemental Formula of [M + H <sup>+</sup> ] <sup>+</sup>	m/z	TIC Peak Area	Chemical Modification vs. CLO
CLO	C <sub>18</sub> H <sub>20</sub> ClN <sub>4</sub>	327.1375 329.1341		
CLO-1 <i>Several peaks</i>	C <sub>18</sub> H <sub>20</sub> ClN <sub>4</sub> O	343.1323 345.1291	1.4 × 10 <sup>8</sup>	CLO + O
CLO-2 <i>Several peaks</i>	C <sub>18</sub> H <sub>20</sub> ClN <sub>4</sub> O <sub>2</sub>	359.1273 361.1238	1.5 × 10 <sup>7</sup>	CLO + 2O
CLO-3 <i>Several peaks</i>	C <sub>18</sub> H <sub>20</sub> ClN <sub>4</sub> O <sub>3</sub>	375.1226 377.1193	2 × 10 <sup>6</sup>	CLO + 3O
CLO-4	C <sub>17</sub> H <sub>18</sub> ClN <sub>4</sub>	313.1218 315.1186	5.6 × 10 <sup>7</sup>	CLO – CH <sub>2</sub>
CLO-5	C <sub>16</sub> H <sub>18</sub> ClN <sub>4</sub>	301.1216	6.8 × 10 <sup>7</sup>	CLO – C <sub>2</sub> H <sub>2</sub>
CLO-6	C <sub>18</sub> H <sub>21</sub> N <sub>4</sub> O	309.1716	1 × 10 <sup>6</sup>	CLO – Cl + OH
CLO-7	C <sub>17</sub> H <sub>18</sub> ClN <sub>4</sub> O	329.1166 331.1136	1.2 × 10 <sup>7</sup>	CLO – Cl + H – CH <sub>2</sub>
CLO-8	C <sub>17</sub> H <sub>19</sub> N <sub>4</sub> O <sub>3</sub>	327.1455	3.2 × 10 <sup>6</sup>	CLO – CH <sub>2</sub> – Cl + OH + 2O
CLO-9	C <sub>18</sub> H <sub>19</sub> N <sub>4</sub> O <sub>2</sub>	323.1504	4 × 10 <sup>6</sup>	CLO – Cl + OH – 2H + O

**Table 3.** HR-MS data of the main photoproducts of CIT after 8 h of irradiation in the presence of WEOM. Percentage of conversion = 33%.

Peak Code	Elemental Formula of [M + H <sup>+</sup> ] <sup>+</sup>	m/z	TIC peak Area	Chemical Modification vs. CIT
CIT	C <sub>20</sub> H <sub>22</sub> ON <sub>2</sub> F	325.1714		
CIT-1 <i>Several peaks</i>	C <sub>20</sub> H <sub>22</sub> O <sub>2</sub> N <sub>2</sub> F	341.1658	1.3 × 10 <sup>9</sup>	CIT + O fragment M – H <sub>2</sub> O
CIT-1 bis <i>Several peaks</i>	C <sub>20</sub> H <sub>22</sub> O <sub>2</sub> N <sub>2</sub> F	341.1658		CIT + O
CIT-2	C <sub>20</sub> H <sub>20</sub> O <sub>2</sub> N <sub>2</sub> F	339.1506	7.2 × 10 <sup>8</sup>	CIT – 2H + O
CIT-3	C <sub>20</sub> H <sub>20</sub> O <sub>3</sub> N <sub>2</sub> F	355.1456	1.3 × 10 <sup>7</sup>	CIT – 2H + 2O
CIT-4	C <sub>19</sub> H <sub>20</sub> ON <sub>2</sub> F	311.1560	2 × 10 <sup>7</sup>	CIT – CH <sub>2</sub>
CIT-5	C <sub>20</sub> H <sub>23</sub> O <sub>2</sub> N <sub>2</sub>	323.1757	2.5 × 10 <sup>8</sup>	CIT – F + OH
CIT-6	C <sub>14</sub> H <sub>19</sub> ON <sub>2</sub>	231.1492	1 × 10 <sup>7</sup>	CIT – aromatic ring
CIT-7 <i>Several peaks</i>	C <sub>14</sub> H <sub>17</sub> O <sub>2</sub> N <sub>2</sub>	245.1287	2.2 × 10 <sup>8</sup>	CIT – aromatic ring-2H+O
CIT-8	C <sub>19</sub> H <sub>20</sub> O <sub>2</sub> N <sub>2</sub> F	327.1509	2 × 10 <sup>8</sup>	CIT – CH <sub>2</sub> + O
CIT-9	C <sub>19</sub> H <sub>20</sub> O <sub>3</sub> N <sub>2</sub> F	343.1456	1 × 10 <sup>7</sup>	CIT – CH <sub>2</sub> + 2O
CIT-10	C <sub>19</sub> H <sub>18</sub> O <sub>2</sub> N <sub>2</sub> F	325.1350	1.2 × 10 <sup>8</sup>	CIT – CH <sub>2</sub> – 2H + O
CIT-11	C <sub>20</sub> H <sub>21</sub> O <sub>4</sub> N <sub>2</sub>	353.1495	8.3 × 10 <sup>6</sup>	CIT – F-2H + OH + 2O
CIT-12	C <sub>20</sub> H <sub>21</sub> O <sub>3</sub> N <sub>2</sub>	337.1546	1.1 × 10 <sup>7</sup>	CIT – F+OH – 2H
CIT-13	C <sub>20</sub> H <sub>23</sub> O <sub>3</sub> N <sub>2</sub>	339.1703	1.2 × 10 <sup>7</sup>	CIT – F+OH +O
CIT-14 <i>Several peaks</i>	C <sub>19</sub> H <sub>21</sub> O <sub>4</sub> N <sub>2</sub>	341.1491	1 × 10 <sup>7</sup>	CIT – CH <sub>2</sub> – F+OH+2O
CIT-15	C <sub>19</sub> H <sub>19</sub> O <sub>3</sub> N <sub>2</sub>	323.1393	1.3 × 10 <sup>6</sup>	CIT – CH <sub>2</sub> – F+OH – 2H+O



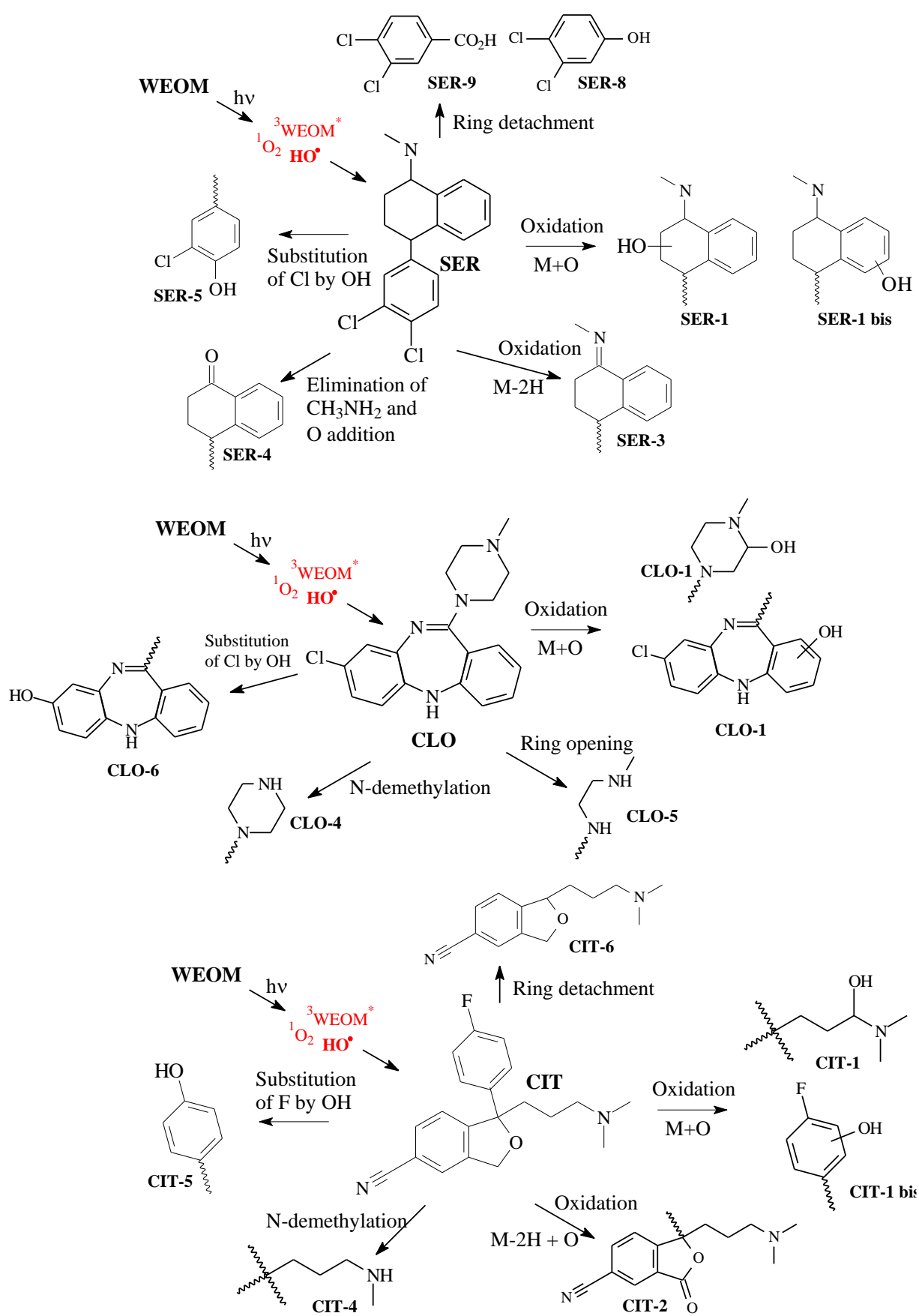


Figure 4. Photodegradation pathways.

Most of the peaks were detected in positive mode. Molecular ion clusters at  $m/z = 322.0753$ ,  $324.0722$ ,  $326.0687$  (SER- and SER-1bis),  $m/z = 343.1323$ ,  $345.1291$  (CLO-1) and peak at  $m/z = 341.1658$  (CIT-1) corresponded all to  $[M + O + H]^+$ . Double O atom addition was also detected for SER and CLO (SER-2, CLO-2) and even triple O atom addition for CLO (CLO-3).

Molecular ion clusters at  $m/z = 304.0647$ ,  $306.0615$ ,  $308.0581$  (SER-3) corresponded to  $[M - 2H + H]^+$  and to the formation of a double bond  $C = C$  or  $C = N$ . Formation of an imine was already proposed [15,16]. In acidic aqueous solution, the imine is expected to be hydrolyzed into the corresponding carbonyl [43]. SER-4 with  $m/z = 291.0330$ ,  $293.0300$ ,  $0295.0266$  corresponding to  $SER - CH_3NH_2 + O$ , could therefore be formed in two steps, first oxidation with the imine  $RR'C = N - CH_3$  formation, then imine hydrolysis into the carbonyl  $RR'C = O$ . In the case of CIT, the elimination of 2 H atoms and addition of O was observed (CIT-2) in accordance with a carbonyl formation [44].

Substitution of the halogen atoms, F or Cl, by OH was observed for the three drugs: SER-5 with  $m/z = 288.1146$  and  $290.1110$ , SER-6 with  $m/z = 270.1481$  [16], CLO-6 with  $m/z = 309.1716$  and CIT-5 with  $m/z = 323.1757$ . Such nucleophilic substitution was often reported in the photolysis of halogenoaromatics and was already observed for the studied drugs [4,44,45].

Interestingly, analysis in negative mode yielded molecular ion clusters at  $m/z = 160.9553$ ,  $162.9524$ ,  $164.9495$  (SER-8) and  $m/z = 188.9507$ ,  $190.9275$ ,  $192.9279$  (SER-9) corresponding to 3,4-dichlorophenol and 3,4-dichlorobenzoic acid, respectively. This result demonstrated that ring detachment took place. The formation of these compounds that show potential toxicity as halogenophenols in general was never reported in the literature to the best of our knowledge. For CIT, the peak at  $m/z = 231.1492$  (CIT-6) may also result from the cleavage of the aromatic ring.

CLO and CIT both underwent N-demethylation as demonstrated by the detection of  $[M - CH_2 + H]^+$  ions (CLO-4 and CIT-4), not observed in the case of SER. This reaction was reported by several authors [2,4,14,44] under various oxidation conditions (UV photolysis, photocatalysis, simulated sunlight irradiation in river water).

Last, in the case of CLO, piperazine ring opening probably took place as shown by the detection of molecular ions cluster at  $m/z = 301.1216$  and  $303.1184$  (CLO-5) corresponding to  $[M - C_2H_2 + H]^+$ . The same compound was observed in the photocatalysis transformation of CLO [4].

Several other photoproducts were found, arising from the combination of the above-described pathways, for instance: SER-7 formed after  $CH_3NH_2$  and Cl elimination, CLO-7 after demethylation and dechlorination, and CIT-10 after demethylation and oxidation.

Given the complexity of the drugs structure and the very oxidant properties of  $HO^\cdot$  radicals, it is highly probable that the attack of drugs by  $HO^\cdot$  took place on several sites (Scheme 1B). Some of M+O compounds (SER-1 and CIT-1) loose  $H_2O$  easily. It is in line with the presence of  $CH(OH)-CH_2$  functionalities in the molecule and with the abstraction of  $H^a$ ,  $H^b$  or  $H^c$ , leading to the aliphatic ring oxidation. N-demethylation observed for CLO and CIT were likely due to abstraction of methyl H atoms.  $HO^\cdot$  radicals could also add to the aromatic rings (d and e in Scheme 1B) to form phenolic structures at the end [2,15,16]. Lastly, the oxidation of the N atom into N-oxide after abstraction of  $H^f$  seems possible [14,44]. The carbon radical produced after H abstraction can either loose a second H atom and yield a double bond or add  $O_2$  to generate a peroxy radical, then a hydroperoxide and further a carbonyl or an alcohol. On the other hand, the addition of  $HO^\cdot$  on the aromatic ring leads to a ring- $HO^\cdot$  adduct and finally to a phenolic compound after abstraction of a ring H-atom elimination. Ring eliminations required the cleavage of a C-C bond and probably involved a complex sequence of processes, the first step of which might have been the abstraction of  $H^c$  by  $HO^\cdot$  (Scheme 1B).

## 2.6. Prediction of Ecotoxicity Assessment

The potential acute ( $LC_{50}$  and  $EC_{50}$ ) and chronic toxicity (ChV) of the 3 target analytes and their photoproducts were predicted using ECOSAR computer program (version 2.0). Based on the predicted ecotoxicity values, SER, CLO, CIT, and their transformation products (TPs), could be classified according to the system established by the Globally Harmonized System of Classification and Labelling of Chemicals (GHS) [46] (Table 4).

**Table 4.** Toxicity classification according to the Globally Harmonized System of Classification and Labelling of Chemicals (GHS). (United Nations, 2011).

Toxicity Range [mg/L]	Class
$LC_{50}/EC_{50}/ChV \leq 1$	Very toxic
$1 > LC_{50}/EC_{50}/ChV \leq 10$	Toxic
$10 > LC_{50}/EC_{50}/ChV \leq 100$	Harmful
$LC_{50}/EC_{50}/ChV > 100$	Not harmful

SER has been found as a moderately toxic compound ( $EC = 20 \text{ mg L}^{-1}$ ) [13]. ECOSAR program predicted that SER and its by-products were very toxic to fish, daphnia and algae, except by-product SER-6, which shows an acute toxicity  $LC_{50}$  for fish up to 10.8 mg/L, and is classified as a harmful compound (Table 5). SER-3 in particular was even more toxic than SER. This finding supports the previously reported observation that treatment of drugs by irradiation can generate products of greater toxicity than the parent compound [47].

**Table 5.** Toxicity predictions for SER and its transformation products using ECOSAR software.

	Acute Toxicity [mg/L]			Chronic Toxicity (ChV) [mg/L]		
	Fish ( $LC_{50}$ )	Daphnid ( $LC_{50}$ )	Algae ( $EC_{50}$ )	Fish ( $LC_{50}$ )	Daphnid ( $LC_{50}$ )	Algae ( $EC_{50}$ )
SER	0.408	0.071	0.028	0.0074	0.0085	0.012
SER-1	0.887	0.147	0.063	0.019	0.017	0.027
SER-2	1.93	0.301	0.154	0.049	0.032	0.059
SER-3	0.078	0.132	0.00072	0.0018	0.021	0.019
SER-4	0.477	0.357	0.839	0.065	0.075	0.408
SER-5	2.10	0.322	0.162	0.0057	0.034	0.064
SER-6	10.8	1.45	0.942	0.435	0.134	0.341
SER-7	1.59	1.13	2.07	0.201	0.201	0.879
SER-8	6.24	3.88	0.566	0.671	0.489	1.46
SER-9	5.96	3.92	5.31	0.692	0.572	1.92

CLO is considered to be a harmful compound, and most of its TPs formed during the degradation process are much less toxic (Table 6). No standardized acute or chronic assay was found in the literature for CLO.

In the case of CIT, data at Table 7 show that the obtained for the parent molecule for fish was about  $4.47 \text{ mg L}^{-1}$ , while  $LC_{50}$  and  $EC_{50}$  were much lower for daphnia and green algae (about  $0.652$  and  $0.360 \text{ mg L}^{-1}$  respectively). The same behavior has been observed for SER and CLO (Tables 5 and 6). In the three cases, the values for chronic toxicity estimated by ECOSAR are lower than those for acute toxicity, suggesting that invertebrates are likely the most sensitive species to these TPs.

Based on the predicted ecotoxicity values, SER and its TPs are toxic or very toxic. CIT is considered as a toxic compound and most of the TPs formed are harmful or not harmful. By contrast, CLO is classified as harmful and most of its by-products formed are not harmful.

**Table 6.** Toxicity predictions for CLO and its transformation products using ECOSAR software.

	Acute Toxicity [mg/L]			Chronic Toxicity (ChV) [mg/L]		
	Fish (LC50)	Daphnid (LC50)	Algae (EC50)	Fish (LC50)	Daphnid (LC50)	Algae (EC50)
CLO	17.7	2.32	1.58	0.764	0.210	0.563
CLO-1	65.2	20.1	6.40	4.58	2.20	8.65
CLO-2	141	15.9	14.6	9.71	1.24	4.67
CLO-3	518	53.1	59.1	47.9	3.76	17.6
CLO-4	23.3	2.98	2.13	1.09	0.263	0.746
CLO-5	26.0	3.29	2.41	1.25	0.287	0.835
CLO-6	155	17.2	16.4	11.3	1.31	5.17
CLO-7	86.0	10.0	8.66	5.38	0.804	2.83
CLO-8	1.65E+3	153	207	206	9.82	57.3
CLO-9	683	67.7	80.5	69.8	4.65	23.4

**Table 7.** Toxicity predictions for CIT and its transformation products using ECOSAR software.

	Acute Toxicity [mg/L]			Chronic Toxicity (ChV) [mg/L]		
	Fish (LC50)	Daphnid (LC50)	Algae (EC50)	Fish (LC50)	Daphnid (LC50)	Algae (EC50)
CIT	4.47	0.652	0.360	0.140	0.065	0.138
CIT-1	48.0	5.86	4.62	2.60	0.493	1.56
CIT-2	21.3	2.77	1.93	0.954	0.247	0.680
CIT-3	249	26.9	27.0	19.7	2.01	8.35
CIT-4	5.88	0.838	0.486	0.199	0.082	0.183
CIT-5	61.6	7.35	6.06	3.58	0.604	2.01
CIT-6	37.2	4.50	3.62	2.08	0.374	1.21
CIT-7	260	27.2	29.1	22.7	1.97	8.80
CIT-8	56.7	6.81	5.54	3.23	0.564	1.85
CIT-9	330	34.7	36.6	28.0	2.53	11.1
CIT-10	28.1	3.56	2.60	1.36	0.310	0.903
CIT-11	636	63.8	74.1	62.6	4.44	21.7
CIT-12	294	31.2	32.	24.4	2.29	9.88
CIT-13	134	15.1	13.9	9.22	1.17	4.43
CIT-14	918	89.3	110	99.2	6.02	31.6
CIT-15	176	19.4	18.8	13.1	1.48	5.88

### 3. Experimental

#### 3.1. Sediment Sampling and Analysis

Sediment was collected in Lake Pamvotis in Ionnina (Epirus Region, Greece). Lake Pamvotis is a shallow Mediterranean urban lake and it occupies an area of 22.8 km<sup>2</sup> with a mean depth of 5 m, and is classified among the few European lakes that are sufficiently old to feature native faunas and floras. It is considered as one of the European biodiversity hot spot and is used for different activities such as recreation, tourism, fishing and irrigation. The regional capital Ioannina to the west and the town of Perama to the north are urban settlements fringing the lake, the remaining of its periphery is composed of farmland. In the form of ditches, two major inflows of surface runoff water occur. One of them drains an agricultural watershed mainly, while the second drains a mixed of urban, rural, agricultural

and industrial land use watershed. An outflow to the north-west controls the water level for flood prevention. The climate in the region is continental, with cold, wet winters ( $<0\text{ }^{\circ}\text{C}$ ) and hot, dry summers ( $>30\text{ }^{\circ}\text{C}$ ). Annual precipitation (1.1–1.2 m) approximates the evaporation of the lake surface. Sediments were collected in September 2019 close to the lake bank (depth 3–7 cm) using an Eckman type sampler [48] and were air-dried. The samples were then stainless-steel sieved over 2 mm to remove large detritus and benthic organisms. The average particle size of sediment was measured in wet dispersions using a laser diffraction particle size analyzer Malvern Mastersizer 3000 and the percentage of organic matter was obtained by loss-on-ignition (dry combustion between 400 and 500  $^{\circ}\text{C}$ ) during 8 h using a high temperature furnace.

### 3.2. Chemicals and Preparation of Solutions

Clozapine (8-Chloro-11-(4-methyl-1-piperazinyl)-5H-dibenzo[b,e][1,4]-diazepine) was purchased from Sigma-Aldrich (quality level 300). Citalopram (1-[3-(dimethylamino)propyl]-1-(4-fluorophenyl)-3H-2-benzofuran-5-carbonitrile, hydrobromide) and sertraline (1S,4S-4-(3,4-dichlorophenyl)-N-methyl-1,2,3,4-tetrahydronaphthalen-1-amine, hydrochloride) were purchased from TCI Tokyo Chemical Industry (Tokyo, Japan). All these drugs had a purity higher than 98%. 2,4,6-Trimethylphenol (certified reference material), furfuryl alcohol (analytical grade), terephthalic acid (98%) and hydroxyterephthalate disodium (97%) were purchased from Sigma-Aldrich and used as received. Acetonitrile and methanol for HPLC were from Carlo-Erba and VWR, respectively. The other reagents were of the highest grade available. Water was purified using a reverse osmosis RIOS 5 and Synergy (Millipore) device (resistivity 18 M $\Omega$ .cm, DOC  $< 0.1\text{ mg L}^{-1}$ ).

Stock solutions of sertraline ( $1 \times 10^{-3}\text{ M}$ ) and citalopram ( $5 \times 10^{-3}\text{ M}$ ) were prepared in purified water while those of clozapine ( $10^{-3}\text{ M}$ ) in water-acetonitrile (95-5, *v/v*). Solubilization was achieved after 24 h stirring at 400 rpm. Stock solutions of 2,4,6-trimethylphenol ( $6.2 \times 10^{-4}\text{ M}$ ), furfuryl alcohol ( $10^{-2}\text{ M}$ ), 2-propanol (2 M), terephthalic acid ( $10^{-2}\text{ M}$ ), and hydroxyterephthalate ( $10^{-3}\text{ M}$ ) were prepared in purified water and stored in the refrigerator in amber glass bottles before use. When necessary, solutions were buffered at pH 7 using a mixture of  $\text{KH}_2\text{PO}_4$  and  $\text{Na}_2\text{HPO}_4$ .

### 3.3. Water Extractable Organic Matter Extraction

Extraction of WEOM was performed by adding 12 g of sediment in 100 mL of purified water adjusted at pH 9.0–9.5 using NaOH and containing  $\text{Na}_2\text{HPO}_4$  ( $6.6 \times 10^{-3}\text{ M}$ ). Suspensions were placed in 200 mL amber glass screw-capped bottles, degassed in a stream of  $\text{N}_2$  during 10 min, closed and stirred during 5 d at 500 rpm at room temperature. After that, the suspensions were filtered using a vacuum filtering flask (Millipore system), first with filters of 5  $\mu\text{m}$  (5VPP, Durapore membrane filters, Millipore) and then with filters of 0.45  $\mu\text{m}$  (HA, Nitrocellulose, Millipore). The obtained WEOM aqueous solutions were characterized in terms of dissolved organic carbon (DOC), UV-Vis absorption, and fluorescence. The procedure was repeated 3 times and all the WEOM solutions were pooled.

### 3.4. DOC Analyses

A Shimadzu 5050 TOC analyser was used to measure the DOC content of solutions. Measurements were made in triplicate.

### 3.5. Optical Analyses

UV-visible analyses of WEOM solutions were conducted on a Varian Cary 3 spectrophotometer in a 1-cm cuvette with purified water as a reference. The absorbances were measured from 250 to 600 nm. The spectral slope ( $S$  in  $\text{nm}^{-1}$ ) was calculated between 275 and 295 nm using Equation (1):

$$A_{\lambda} = A_{\lambda 0} \times e^{-S(\lambda - \lambda 0)} \quad (1)$$

where  $A_\lambda$  and  $A_{\lambda_0}$  are the absorbances at 295 and 275 nm, respectively [48]. The specific absorption coefficient at 254 nm ( $SUVA_{254}$  in  $L\ mg^{-1}\ m^{-1}$ ) was calculated by dividing the absorbance at 254 nm by the DOC concentration in  $mg\ L^{-1}$ . The ratio  $E_2/E_3$  was calculated by dividing the absorbance at 250 nm by the absorbance at 365 nm, where  $E_2$  and  $E_3$  are the absorbance at 250 and 365 nm, respectively. The percentage of aromaticity [49] and the average molecular weight (Mw) of WEOM [50] were estimated following Equations (2) and (3), respectively:

$$\text{percent aromaticity} = 6.52 \times SUVA_{254} + 3.63 \quad (2)$$

$$Mw = 0.315 \times e^{(4.96/(-1.72 + E_2/E_3))} \quad (3)$$

The three-dimensional fluorescence spectrum was recorded using a Perkin Elmer LS 55 Luminescence Spectrometer fitted with a 1-cm quartz cuvette. The bandwidths were set to 10 nm for excitation and 10 nm for emission. A series of emission scans between 250 and 600 nm were collected over excitation wavelengths between 240 and 450 nm at 10 nm increments. The fluorescence index (FI) was obtained by dividing the emission intensity at 450 nm by the emission intensity at 500 nm for excitation at 370 nm [51] and the biological index (BIX) was calculated as the ratio of emission intensity at 380 nm to 430 nm with excitation at 310 nm [52].

### 3.6. Irradiations

Irradiations were carried out in a device equipped with six fluorescent tubes (Sylvania, F15 W/350BL) emitting polychromatic light between 300 and 500 nm with a maximum at 365 nm (Supplementary Figure S5). Ten mL of solutions were irradiated in a Pyrex glass reactor (14 mm i.d.) let open to air. Drugs ( $5 \times 10^{-6}$  M) were irradiated alone in purified water buffered to pH 7, or in presence of WEOM ( $5\ mgC\ L^{-1}$ ). Dark control experiments were also performed in order to determine whether adsorption of drugs on WEOM takes place. For this, starting solutions of each drug and WEOM ( $5\ mgC\ L^{-1}$ ) covered with aluminum foil were kept in the dark and aliquots (5 mL) were withdrawn from the bottles after 1, 2 and 3 h to determine the drug concentration. Probe molecules (2,4,6-trimethylphenol at  $5 \times 10^{-6}$  M, furfuryl alcohol at  $10^{-4}$  and  $5 \times 10^{-5}$  M, or terephthalic acid at  $10^{-5}$  M) were also irradiated alone in pH 7 buffered purified water, or in presence of WEOM ( $5\ mgC\ L^{-1}$ ). When drugs, or probe molecules were irradiated in the presence of WEOM, the reactants were mixed with vortex during 3 min, poured in the reactor and immediately after lamps were turned on. At given irradiation times, small aliquots were taken for HPLC analyses. These data were used to determine the initial rates of phototransformation. The number of photons received by the 10 mL of solutions in the cylindrical reactor was measured using a radiometer QE65000 from Ocean Optics coupled to chemical actinometry using metamitron [53]. The rate of light absorption of WEOM ( $5\ mgC\ L^{-1}$ ),  $R_a^{WEOM}$  was equal to  $(7.2 \pm 0.7) \times 10^{-6}\ E\ s^{-1}$  (Supplementary Figure S1) The screen effect of WEOM on drugs was calculated as described in SI-Text 1. All the rates of photodegradation obeyed an apparent first order kinetics, and the apparent first order reaction rate constants ( $k$  in  $s^{-1}$ ) were calculated according to Equation (4):

$$\ln C_t/C_0 = -k \times t \quad (4)$$

where  $C_t$  is the concentration of the chemical at the irradiation time  $t$  and  $C_0$  is the initial concentration. Irradiations were duplicated.

### 3.7. HPLC Analyses

HPLC analyses were carried out at 25 °C on an Alliance (Waters, Milford, MA, USA) apparatus equipped with a photodiode array detector (model 2998), fluorescence detector (model 2475) and two pumps (Waters 2695). Separation was achieved on a reverse phase Nucleodur, Macherey-Nagel  $C_8$  column ( $5\ \mu m$ ,  $150\ mm \times 4.6\ mm$ ) equipped with a 4/3 pre-column made of the same material. The binary solvent system used was com-



posed of solvent A (100% MeOH) and solvent B (water acidified by 0.03% of H<sub>3</sub>PO<sub>4</sub>). The best separation of psychoactive drugs was obtained with the following gradient: from 0–20 min, 20% A, then from 20–27 min, 80% A and return to 20% A. The solvent flow was 0.75 mL·min<sup>-1</sup> and the volume injection was 25 µL. The eluent was a mixture of 20% MeOH and 80% water acidified with orthophosphoric acid (0.1%) for the experiments with terephthalic acid and furfuryl alcohol while a mobile phase of 50% acetonitrile and 50% acidified water was used for the experiments with 2,4,6-trimethylphenol. Hydroxyterephthalate concentration was measured by fluorescence ( $\lambda_{exc} = 320$  nm and  $\lambda_{em} = 430$  nm) using a calibration curve (Supplementary Figure S3). Analyses were duplicated.

Psychoactive drugs photoproducts were identified by HRMS performed on an Orbitrap Q-Exactive (Thermo Scientific, Waltham, MA, USA) coupled to an UHPLC Ultimate 3000 RSLC (Thermo Scientific, Waltham, MA, USA) equipped with an Acquity Phenomenex (2.1 mm × 100 mm, 1.7 µm particle size) analytical column (Waters, Milford, MA, USA). The aqueous solvent (A) consisted of a mixture of 0.1% formic acid and the organic phase (B) was acetonitrile. The separation was achieved with a gradient program consisting of 0–7.5 min 5%, 7.5–8.5 min 99% of the mobile phase B. After 8.5 min the gradient was returned to the initial conditions and analytical column was reconditioned for 3.5 min. The flow rate was set to 0.45 mL·min<sup>-1</sup>. The injection volume was 20 µL. The mass spectrometer operated in the positive and negative (ESI) electrospray ionization mode. The system was controlled by Xcalibur 2.2 (Thermo Fisher Scientific software, Waltham, MA, USA). The spray voltage was 3 kV for the positive and negative mode. For all proposed elemental formula, the error between the measured mass and the exact mass was less than 5 ppm.

### 3.8. Ecotoxicity Assessment

The ecotoxicity of the 3 target analytes and their by-products were predicted using ECOSAR program (v 2.0). ECOSAR uses a quantitative structure-activity relationship approach to predict the toxicity of a molecule based on its structure. The relevant endpoints are the acute toxicity, LC<sub>50</sub> (concentration of tested compound that is lethal to half of fish and daphnia population after 96 h and 48 h of exposure, respectively) and EC<sub>50</sub> (concentration of tested compound that inhibits the growth % of green algae after 96 h of exposure). The chronic toxicity values (ChV) of the drugs and their by-products also were predicted using the same program, for freshwater fish, daphnid and algae as well. Concerning accuracy, a compound is considered more toxic than another if the expected values vary by at least an order of magnitude [54]. The program (v 2.0) is freely available at the website: <https://www.epa.gov/tsca-screening-tools/ecological-structure-activity-relationships-ecosar-predictive-model> (accessed on 1 March 2021).

## 4. Conclusions

We showed that the water-soluble organic constituents of sediments are able to induce the oxidation of drugs under simulated solar light. The scavenging techniques revealed that hydroxyl radicals were the major contributors of these oxidations even though irradiation of WEOM led to other oxidant species. Thirty-five photoproducts were detected and identified by means of high-resolution mass spectrometry. Some of the proposed degradation pathways are found to be in common with all three drugs (oxidation through O addition or substitution of the halogen by OH), some are shared by only two of them (ring detachment or N-demethylation), while others are specific to a particular drug (dehydrogenation, N-elimination or ring opening). This study demonstrates that the fate of sertraline, clozapine and citalopram in lakes can be affected by sedimental organic constituents through photodegradation and that many by-products potentially toxic can be formed. Based on ECOSAR software, ecotoxicity assessments showed that toxic and very toxic by-products can be produced for sertraline, while harmful and not harmful TPs could be formed after WEOM mediated photodegradation of citalopram and clozapine.



**Supplementary Materials:** The following are available online, Figure S1: Photodegradation of 2,4,6-trimethylphenol in the presence of WEOM, Figure S2: Photodegradation of furfuryl alcohol in the presence of WEOM, Figure S3: Formation of hydroxyterephthalic acid upon irradiation of terephthalic acid in the presence of WEOM, Figure S4: Adsorption of drugs to sediment, Figure S5: Irradiance of the fluorescent tubes, Table S1: Rate constants of drugs photodegradation in the presence of WEOM; Text Section S1: Screen effect calculation.

**Author Contributions:** Conceptualization, V.S., C.R.; methodology, C.R.; software, C.J.-H.; validation, V.S., C.R.; formal analysis, C.J.-H.; investigation, C.J.-H.; resources, V.S., C.R., C.J.-H.; data curation, C.J.-H.; writing—original draft preparation, C.J.-H.; writing—review and editing, C.R.; supervision, C.R.; project administration, V.S., C.R.; funding acquisition, V.S., C.R. All authors have read and agreed to the published version of the manuscript.

**Funding:** This paper is part of a project that received funding from the European Union’s Horizon 2020 research and innovation programme under the Marie Skłodowska-Curie grant agreement no. 765,860 (Aquality).

**Acknowledgments:** The authors would like to thank Martin Lereboure (Engineer CNRS) and Frédéric Emmenegger (Tech CNRS) for UHPLC-MS analyses and Guillaume Voyard (Engineer CNRS) for assistance in HPLC.

**Conflicts of Interest:** The authors declare no conflict of interest. The funders had no role in the design of the study; in the collection, analyses, or interpretation of data; in the writing of the manuscript, or in the decision to publish the results.

**Sample Availability:** Samples of sediments are available from the authors.

## References

1. Calisto, V.; Esteves, V. Psychiatric pharmaceuticals in the environment. *Chemosphere* **2009**, *77*, 1257–1274. [[CrossRef](#)] [[PubMed](#)]
2. Skibiński, R.; Trawiński, J.; Komsta, Ł.; Bajda, K. Characterization of forced degradation products of clozapine by LC-DAD/ESI-Q-TOF. *J. Pharm. Biomed. Anal.* **2016**, *131*, 272–280. [[CrossRef](#)] [[PubMed](#)]
3. Trawiński, J.; Skibiński, R. Studies on photodegradation process of psychotropic drugs: A review. *Environ. Sci. Pollut. Res.* **2017**, *24*, 1152–1199. [[CrossRef](#)] [[PubMed](#)]
4. Trawiński, J.; Skibiński, R. Rapid degradation of clozapine by heterogeneous photocatalysis. Comparison with direct photolysis, kinetics, identification of transformation products and scavenger study. *Sci. Total. Environ.* **2019**, *665*, 557–567. [[CrossRef](#)]
5. Delorenzo, M.; Fleming, J. Individual and mixture effects of selected pharmaceuticals and personal care products on the marine phytoplankton species *Dunaliella tertiolecta*. *Arch. Environ. Contam. Toxicol.* **2008**, *54*, 203–210. [[CrossRef](#)]
6. Dietrich, S.; Ploessl, F.; Bracher, F.; Laforsch, C. Single and combined toxicity of pharmaceuticals at environmentally relevant concentrations in *Daphnia magna*—A multigenerational study. *Chemosphere*. **2010**, *79*, 60–66. [[CrossRef](#)]
7. Godoy, A.; de Oliveira, A.; Silva, J.; Azevedo, C.; Domingues, I.; Nogueira, A.; Kummrow, F. Single and mixture toxicity of four pharmaceuticals of environmental concern to aquatic organisms, including a behavioral assessment. *Chemosphere* **2019**, *235*, 373–382. [[CrossRef](#)]
8. Hossain, M.; Kubec, J.; Guo, W.; Roje, S.; Ložek, F.; Grabicová, K.; Randák, T.; Kouba, A.; Buřič, M. A combination of six psychoactive pharmaceuticals at environmental concentrations alter the locomotory behaviour of clonal marbled crayfish. *Sci. Total. Environ.* **2021**, *751*, 141383. [[CrossRef](#)]
9. Gonzales-Rey, M.; Mattos, J.; Piazza, C.; Bainy, A.; Bebianno, M. Effects of active pharmaceutical ingredients mixtures in mussel *Mytilus galloprovincialis*. *Aquat. Toxicol.* **2014**, *153*, 12–26. [[CrossRef](#)]
10. Franzellitti, S.; Buratti, S.; Bowen, D.; Haddad, S.; Chambliss, C.; Brooks, B. A multibiomarker approach to explore interactive effects of propranolol and fluoxetine in marine mussels. *Environ. Pollut.* **2015**, *205*, 60–69. [[CrossRef](#)]
11. Ding, J.; Lu, G.; Li, Y. Interactive effects of selected pharmaceutical mixtures on bioaccumulation and biochemical status in crucian carp (*Carassius auratus*). *Chemosphere* **2016**, *148*, 21–31. [[CrossRef](#)]
12. Villain, J.; Minguez, L.; Halm-Lemeille, M.; Durrieu, G.; Bureau, R. Acute toxicities of pharmaceuticals toward green algae. mode of action, biopharmaceutical drug disposition classification system and quantile regression models. *Ecotoxicol. Environ. Saf.* **2016**, *124*, 337–343. [[CrossRef](#)]
13. Calza, P.; Jiménez-Holgado, C.; Cocha, M.; Chrimatopoulos, C.; dal Bello, F.; Medana, C.; Sakkas, V. Study of the Photoinduced Transformations of Sertraline in Aqueous Media. *Sci. Tot. Environ.* **2021**, *756*, 143805. [[CrossRef](#)]
14. Kwon, J.W.; Armbrust, K.L. Degradation of citalopram by simulated sunlight. *Environ. Toxicol. Chem.* **2005**, *24*, 1618–1623. [[CrossRef](#)]
15. Gornik, T.; Vozic, A.; Heath, E.; Trontelj, J.; Roskar, R.; Zigon, D.; Vione, D.; Kosjek, T. Determination and photodegradation of sertraline residues in aqueous environment. *Environ. Pollut.* **2020**, *256*, 113431. [[CrossRef](#)]

16. Jakimska, A.; Śliwka Kaszyńska, M.; Nagórski, P.; Kot Wasik, A.; Namieśnik, J. Environmental Fate of Two Psychiatric Drugs, Diazepam and Sertraline: Phototransformation and Investigation of their Photoproducts in Natural Waters. *J. Chromatogr. Sep. Tech.* **2014**, *5*, 1000253/1–1000253/12. [[CrossRef](#)]
17. Cooper, W.J.; Zika, R.G.; Petasne, R.G.; Plane, J.M. Photochemical formation of hydrogen peroxide in natural waters exposed to sunlight. *Environ. Sci. Technol.* **1988**, *22*, 1156–1160. [[CrossRef](#)]
18. Zepp, R.G.; Schlotzhauer, P.F.; Sink, R.M. Photosensitized Transformations Involving Electronic Energy Transfer in Natural Waters: Role of Humic Substances. *Environ. Sci. Technol.* **1985**, *19*, 74–81. [[CrossRef](#)]
19. Peterson, B.M.; McNally, A.M.; Cory, R.M.; Thoemke, J.D.; Cotner, J.B.; McNeill, K. Spatial and temporal distribution of singlet oxygen in Lake Superior. *Environ. Sci. Technol.* **2012**, *46*, 7222–7229. [[CrossRef](#)]
20. Canonica, S.; Urs, J.; Stemmler, K.; Hoigné, J. Transformation Kinetics of Phenols in Water: Photosensitization. *Environ. Sci. Technol.* **1995**, *29*, 1822–1831. [[CrossRef](#)]
21. Vaughan, P.P.; Blough, N.V. Photochemical formation of hydroxyl radical by constituents of natural waters. *Environ. Sci. Technol.* **1998**, *32*, 2947–2953. [[CrossRef](#)]
22. Mopper, K.; Zhou, X. Hydroxyl radical photoproduction in the sea and its potential impact on marine processes. *Science* **1990**, *250*, 661–664. [[CrossRef](#)]
23. Vione, D.; Minella, M.; Maurino, V.; Minero, C. Indirect photochemistry in sunlit surface waters: Photoinduced production of reactive transient species. *Chem. A Eur. J.* **2014**, *20*, 10590–10606. [[CrossRef](#)]
24. Koelmans, A.A.; Prevo, L. Production of dissolved organic carbon in aquatic sediment suspensions. *Water Res.* **2003**, *37*, 2217–2222. [[CrossRef](#)]
25. Chen, M.; Hur, J. Pre-treatments, characteristics, and biogeochemical dynamics of dissolved organic matter in sediments: A review. *Water Res.* **2015**, *79*, 10–25. [[CrossRef](#)]
26. Nkhili, E.; Boguta, P.; Bejger, R.; Guyot, G.; Sokołowska, Z.; Richard, C. Photosensitizing properties of water-extractable organic matter from soils. *Chemosphere* **2014**, *95*, 317–323. [[CrossRef](#)] [[PubMed](#)]
27. Ritchie, J.C. Organic Matter Content in Sediments of Three Navigation Pools along the Upper Mississippi River. *J. Freshw. Ecol.* **1988**, *4*, 343–349. [[CrossRef](#)]
28. Romero, J.; Kagalou, I.; Imberger, J.; Hela, D.; Kotti, M.; Bartzokas, A.; Albanis, T.; Evmirides, N.; Karkabounas, S.; Papagiannis, J.; et al. Seasonal water quality of shallow and eutrophic Lake Pamvotis, Greece: Implications for restoration. *Hydrobiologia* **2002**, *474*, 91–105. [[CrossRef](#)]
29. Touka, A.; Vareli, K.; Igglezou, M.; Monokrousos, N.; Alivertis, D.; Halley, J.; Hadjikakou, S.; Frillingos, S.; Sainis, I. Ancient European Lakes: Reservoirs of Hidden Microbial Diversity? The Case of Lake Pamvotis (NW Greece). *Open J. Ecol.* **2008**, *8*, 537–578. [[CrossRef](#)]
30. Frogley, M.R.; Huw, I.G.; Heaton, T.H.E. Historical Biogeography and Late Quaternary Environmental Change of Lake Pamvotis, Ioannina (North-Western Greece): Evidence from Ostracods. *J. Biogeogr.* **2001**, *28*, 745–756. [[CrossRef](#)]
31. Daskalou, V.; Polona, V.; Gregor, M.; Constantine, S. Recent Environmental Changes in the Shallow Lake Pamvotis (NW Greece): Evidence from Sedimentary Organic Matter, Hydrocarbons, and Stable Isotopes. *Arch. Environ. Contam. Toxicol.* **2009**, *57*, 21–31. [[CrossRef](#)]
32. Cole, R.A.; Weigmann, D.L. Relationships among Zoobenthos, Sediments, and Organic Matter in Littoral Zones of Western Lake Erie and Saginaw Bay. *J. Great Lakes Res.* **1983**, *9*, 568–581. [[CrossRef](#)]
33. Lara, R.J.; Gomez, E.A.; Pucci, A.E. Organic Matter, Sediment Particle Size and Nutrient Distributions in a Sewage Affected Shallow Channel. *Mar. Pollut. Bull.* **1985**, *16*, 360–364. [[CrossRef](#)]
34. Fu, P.; Wu, F.; Liu, C.Q.; Wei, Z.; Bai, Y.; Liao, H. Spectroscopic characterization and molecular weight distribution of dissolved organic matter in sediment porewaters from Lake Erhai, Southwest China. *Biogeochemistry* **2006**, *81*, 179–189. [[CrossRef](#)]
35. Coble, P.G. Marine optical biogeochemistry: The chemistry of ocean color. *Chem. Rev.* **2007**, *107*, 402–418. [[CrossRef](#)]
36. Xu, H.; Zou, L.; Guan, D.; Li, W.; Jiang, H. Molecular Weight-Dependent Spectral and Metal Binding Properties of Sediment Dissolved Organic Matter from Different Origins. *Sci. Tot. Environ.* **2019**, *665*, 828–835. [[CrossRef](#)]
37. Rosario-Ortiz, F.L.; Canonica, S. Probe Compounds to Assess the Photochemical Activity of Dissolved Organic Matter. *Environ. Sci. Technol.* **2016**, *50*, 12532–12547. [[CrossRef](#)]
38. McKay, G.; Huang, W.; Romera-Castillo, C.; Crouch, J.E.; Rosario-Ortiz, F.L.; Jaffé, R. Predicting Reactive Intermediate Quantum Yields from Dissolved Organic Matter Photolysis Using Optical Properties and Antioxidant Capacity. *Environ. Sci. Technol.* **2017**, *51*, 5404–5413. [[CrossRef](#)]
39. Haag, W.R.; Hoigné, J.R.; Gassman, E.; Braun, A.M. Singlet oxygen in surface waters Part I: Furfuryl alcohol as a trapping agent. *Chemosphere* **1984**, *13*, 631–640. [[CrossRef](#)]
40. Wilkinson, F.; Helman, W.P.; Ross, A.B. Rate constants for the decay and reactions of the lowest electronically excited singlet state of molecular oxygen in solution. An expanded and revised compilation. *J. Phys. Chem. Ref. Data* **1995**, *24*, 663–677. [[CrossRef](#)]
41. Page, S.E.; Arnold, W.A.; McNeill, K. Terephthalate as a probe for photochemically generated hydroxyl radical. *J. Environ. Monit.* **2010**, *12*, 1658–1665. [[CrossRef](#)] [[PubMed](#)]
42. Buxton, G.V.; Greenstock, C.L.; Helman, W.P.; Ross, A.B. Critical review of rate constants for reactions of hydrated electrons, hydrogen atoms and hydroxyl radicals in aqueous solution. *J. Phys. Chem. Ref. Data* **1988**, *17*, 513–886. [[CrossRef](#)]

43. Shen, L.Q.; Beach, E.S.; Xiang, Y.; Tshudy, D.J.; Khanina, N.; Horwitz, C.P.; Bier, M.E.; Collins, T.J. Rapid Biomimetic Degradation in Water of the Persistent Drug Sertraline by TAML Catalysts and Hydrogen Peroxide. *Environ. Sci. Technol.* **2011**, *45*, 7882–7887. [[CrossRef](#)] [[PubMed](#)]
44. Osawa, R.A.; Carvalho, A.P.; Monteiro, O.C.; Oliveira, M.C.; Florêncio, M.H. Transformation products of citalopram: Identification, wastewater analysis and in silico toxicological assessment. *Chemosphere* **2019**, *217*, 858–868. [[CrossRef](#)]
45. Hörsing, M.; Kosjek, T.; Andersen, H.R.; Heath, E.; Ledin, A. Fate of Citalopram during Water Treatment with O<sub>3</sub>, ClO<sub>2</sub>, UV and Fenton Oxidation. *Chemosphere* **2012**, *89*, 129–135. [[CrossRef](#)]
46. United Nations. *Globally Harmonized System of Classification and Labelling of Chemical (GHS)*, 4th ed.; United Nations Publications: New York, NY, USA, 2011.
47. Brown, A.; Challis, J.; Wong, C.; Hanson, M. Selective serotonin reuptake inhibitors and  $\beta$ -blocker transformation products may not pose a significant risk of toxicity to aquatic organisms in wastewater effluent-dominated receiving waters. *Integr. Environ. Assess. Manag.* **2015**, *11*, 618–639. [[CrossRef](#)]
48. Dimitra, G.H.; Lambropoulou, D.A.; Konstantinou, I.K.; Albanis, T.A. Environmental Monitoring and Ecological Risk Assessment for Pesticide Contamination and Effects. in Lake Pamvotis, northwestern Greece. *Environ. Toxicol. Chem.* **2005**, *24*, 1548–1556. [[CrossRef](#)]
49. Weishaar, J.L.; Aiken, G.R.; Bergamaschi, B.A.; Fram, M.S.; Fujii, R.; Mopper, K. Evaluation of Specific Ultraviolet Absorbance as an Indicator of the Chemical Composition and Reactivity of Dissolved Organic Carbon. *Environ. Sci. Technol.* **2003**, *37*, 4702–4708. [[CrossRef](#)]
50. Lou, T.; Xie, H. Photochemical Alteration of the Molecular Weight of Dissolved Organic Matter. *Chemosphere* **2006**, *65*, 2333–2342. [[CrossRef](#)]
51. McKnight, D.M.; Boyer, E.W.; Westerhoff, P.K.; Doran, P.T.; Kulbe, T.; Andersen, D.T. Spectrofluorometric Characterization of Dissolved Organic Matter for Indication of Precursor Organic Material and Aromaticity. *Limnol. Oceanogr.* **2001**, *46*, 38–48. [[CrossRef](#)]
52. Huguet, A.; Vacher, L.; Relexans, S.; Saubusse, S.; Froidefond, J.M.; Parlanti, E. Properties of Fluorescent Dissolved Organic Matter in the Gironde Estuary. *Org. Geochem.* **2009**, *40*, 706–719. [[CrossRef](#)]
53. Kouras-Hadef, S.; de Sainte Claire, P.; ter Halle, A.; Amine-Khodja, A.; Richard, C. The Role of Triplet State Keto-Enol Tautomerism in the Photodeamination of Metamitron. *J. Phys. Chem. A* **2011**, *115*, 14397–14406. [[CrossRef](#)]
54. Mayo-Bean, K.; Moran, K.; Meylan, B. *Methodology Document for the ECological Structure-Activity Relationship Model (ECOSAR) Class Program*; US-EPA: Washington, DC, USA, 2012.